Calibration and Normalization of Time Domain Network Analyzer Measurements

Tom Dhaene, Luc Martens, and Daniël De Zutter

Abstract—**In this paper, we present a new advanced calibration and normalization procedure for time domain reflection and transmission (TDR/T-) measurements. Our approach reduces the systematic error of the time domain network analyzer significantly. The error correction is based on a twoport error model, as already known for network analyzers. All measurements proceed in the time domain, while the error correction itself proceeds completely in the frequency domain. This new algorithm calculates the normalized (time domain) TDR/T-pictures as well as the calibrated (frequency domain) S-parameters.**

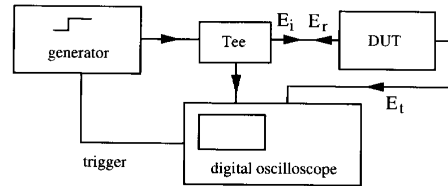

Fig. 1. Time domain network analyzer.

I. Introduction

A. General

SEVERAL modern measurement techniques are based on the reflection and the transmission of time domain signals, such as SONAR (sound navigation and ranging), RADAR (radio detection and ranging), NMR (nuclear magnetic resonance), seismographic measurements, and so on. Usually, a fast time domain signal is emitted or injected in a device or medium under test and the reflected and the transmitted signals are observed. The time domain network analyzer (TDNA) is based on the same principles. The basic set-up is depicted in Fig. 1. A voltage pulse or step E_i is injected in the device under test (DUT). A part of the injected signal will be reflected at the discontinuities of the structure. The injected E_i and the reflected E_r voltage waves constitute the time domain reflection picture (TDR-picture or reflectogram). The voltage wave E_t in transmission constitutes the time domain transmission picture (TDT-picture). A broadband digital oscilloscope captures these pictures. The bandwidth of the digital oscilloscope, the rise time of the injected signal and the filtering characteristics of the measurement cables determine the accuracy and the resolution of the TDR/T-system. The bandwidth of modern TDR/T measurement systems is competitive with the frequency range of traditional network analyzers. Recently, some broadband oscilloscopes up to 150 GHz are described in literature [1].

Quite often TDR-pictures are used to localize errors in a DUT, and to determine the impedance level of transmission structures. The behavior of discontinuities is easily detected by simple waveform examination. The TDR-measurements are also used to determine the return loss, the standing wave ratio (VSWR), the reflection coefficient, and the scattering parameters S_{11} and S_{22} of a DUT. On the other hand, the TDT-measurements are used to determine the propagation time, the length, the gain or loss, the crosstalk, the transmission coefficient, and the scattering parameters S_{21} and S_{12} of a two–port DUT. Up to now, time domain data are often obtained without precision calibration techniques, which limits their utility. Different measurement results are obtained from different measurement set-ups (this even remains true for the same type of equipment of the same company) due to the non-ideal behavior of the equipment. This is well-known and documented for frequency domain measurements with a network analyzer. This problem can be circumvented by a *calibration* procedure which transforms raw measurement data into corrected ones, eliminating (some of) the systematic errors introduced by the measurement set-up. To do so we use so-called error models for the TDR/T-measurements. The error models are fully characterized by measuring a set of well-defined broadband calibration standards. The calibration procedure permits to calculate the corrected time domain answer for arbitrary input steps (with a desired rise time). This is called *normalization* of the TDR-picture.

B. Literature—Review

In the beginning of the thirties, the TDR/T-technique was already used for the fault location in cables [2]. The following decades, the measurement methods were remarkably refined. Nowadays, time domain reflection and transmission measurements are used in a wide range of applications (fault location in cables, study of the dielectric constant of materials, impedance control of quasi-matched interconnection structures,...) [3]–[11] thanks to modern fast pulse and step generators, advanced digital measurement equipment, powerful signal processing techniques and fast and cheap computers.

The characterization of non-linear components in the time domain is discussed in [12]. The fundamental principles of the time domain network analyzer are extensively described in [13]–[16]. No error correction is done in these papers, and

Manuscript received January 19, 1993; revised June 7, 1993. This work was supported in part by grants from the IWONL and the NFWC.
The authors are with the Laboratory of Electromagnetism and Acoustics, University of Ghent, Sint-Pietersnieuwstraat 41, 9000 Ghent, Belgium.
IEEE Log Number 9216056..

0018-9480/94$04.00 © 1994 IEEE

airlines and time windows are used to remove the secondary reflections of the DUT. This approach only gives good results in specific situations (quasi-matched). More sophisticated calibration algorithms and error correcting methods must be used to study more general structures. Scott and Smith [17]–[18] described some important error sources of oneport networks and they corrected the errors produced by the time base of the oscilloscope. They also developed a new oneport calibration method. All calibration standards were idealized. Later on, this oneport method was extended by Su and Riad [19], but the TDR-pictures were not normalized. The TDR/T-measurement systems of Hewlett Packard [20]–[22] use a fairly simple reflection and transmission calibration method (firmware). Their method has a lot of constraints: all calibration standards are idealized, and airlines and time windows must be used to separate primary and secondary reflections. No S-parameters are calculated. In fact, this is not a real twoport calibration algorithm (see the Appendix for more details).

Sophisticated calibration techniques are generally adopted for frequency domain measurements (SOLT-, TRL-, LRL-, ... calibration techniques) [23], while on the other hand, up to now, similar calibration and normalization procedures are seldomly used for standard time domain measurements. Recently, some more advanced time domain calibration techniques are described. The thru-match-short (TMS) and the thru-reflect-line (TRL) calibration techniques are used in [24], [25] respectively to characterize twoport networks in the time domain. The proposed frequency domain error models do not have an isolation factor or crosstalk factor, and some of the reference standards are supposed to be ideal (lossless, no parasitic effects,...). In [25] the directivity error factor is omitted. The algorithms described in [24], [25] need two step or pulse generators and two samplers.

C. New Approach

In this paper, we present a new advanced data-processing technique for the error correction of the time domain network analyzer. We use a rather inexpensive and simple measurement set-up which consists of only one step or pulse generator and two samplers. Our calibration and normalization software package TTRECS (time domain transmission and reflection calibration software) is not restricted to the calculation of the normalized time domain signals (TDR/T-pictures), but the corrected frequency domain S-parameters can also be calculated. We use popular frequency domain error models [23] to correct the oneport and twoport time domain measurements [26]. These error models are fully characterized by measuring a set of precisely known SOLT- (short, open, load, thru) calibration standards. The devices under test are supposed to be linear. First, the discretized time domain data are transformed to the frequency domain. Then, the frequency domain data are corrected mathematically and the scattering parameters of the DUT are calculated. Afterwards, the corrected data are transformed back to the time domain. So, the normalized time domain responses of an arbitrary RF-burst, or a step or pulse with a predefined rise time can be calculated.

The reader must be aware of the fact that the proposed technique uses already well-known techniques for frequency domain measurements [23]. The explicit purpose of this paper is to show that application of these methods to time domain measurements substantially enhances the obtained results while retaining some of the prominent features of TDR/T such as ease of use and relative inexpensive equipment.

II. Calibration and Normalization

In this section we discuss the calibration and the normalization procedure for time domain measurements.

A. Error Correction: Introduction

Calibration and normalization of the time domain network analyzer reduce the errors and the uncertainties of time domain reflection and transmission measurements significantly, and guarantee an enhanced measurement accuracy. We use well-known frequency domain error models [23] to correct the oneport and twoport time domain measurements. These error models compensate the linear systematic errors caused by the generator, the oscilloscope, the cables and connectors. The real (imperfect) TDR(/T)-measurement set-up is modeled as a perfect TDR(/T)-measurement system in combination with a one- or twoport error model. This calibration method is based on the calibration algorithms used for the frequency domain network analyzer. The accuracy of the measurements is limited by the noise level of the measurement equipment, by the sampling rate, and by the accuracy to which the calibration standards are known.

The calibration and the normalization procedure of the time domain network analyzer proceeds in three steps. *First,* the measured time domain signals (SOLT-reference standards and DUT) are transformed to the frequency domain. We use the "Enhanced Spectral Resolution Fast Fourier Transform" [27] to transform the step-like time domain signals. *Secondly,* the parameters of the error network are determined in the frequency domain, the calibrated S-parameters of the DUT are calculated and the measured data are corrected and normalized to the desired rise time. The normalized bandwidth is determined and limited by the normalized rise time. The error correction process is based on advanced data processing techniques [27]–[29]. Since the TDR/T-pictures still contain some useful information beyond the cut-off frequency of the oscilloscope, the high frequency components of the signals may be "pumped up" to compensate for (skin-effect) cable losses or other unwanted filtering effects. Increasing the signal level beyond the 3 dB-bandwidth of the measured signal means that the noise level will increase and the S/N ratio will decrease. This is shown in Fig. 2 [21]. An increased 3 dB-bandwidth of the signal corresponds with a decreased rise time of the injected step. The spatial resolution of the TDR/T-pictures will improve by decreasing the rise time, and at the same time the 3 dB-bandwidth and the noise content of the normalized measurement will increase. The minimal possible rise time is determined by the sampling rate of the oscilloscope (Nyquist criterion) and the signal/noise-ratio of the measurements. *Finally,* the normalized frequency domain

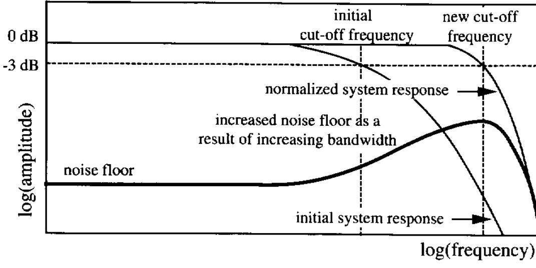

Fig. 2. Normalized system response with enhanced bandwidth [21].

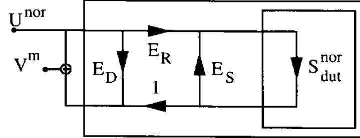

Fig. 3. Flow graph of one-port error model.

data are transformed back to the time domain. So, the time domain response of an arbitrary RF-burst, a step or pulse with a predefined rise time can be found.

B. Oneport Error Model for Time Domain Reflection Measurements

The (voltage) flow chart used for reflection measurements is depicted in Fig. 3. The real, imperfect reflectometer is modeled as an ideal reflectometer, which consists of a normalized voltage source, and an error network, which groups the linear systematic errors of the real measurement set-up (losses, mismatches, delays, ...). The normalized voltage source has an internal impedance of $R\ \Omega$ (quite often 50 Ω), and it generates a normalized voltage step with amplitude $2U^{\rm nor}$ and rise time $t_r^{\rm nor}$. The error model has three relevant error factors:

1) E_D the directivity,
2) E_S the source impedance match,
3) E_R the reflection frequency response.

These error factors can be seen as S-parameters (reference impedance = internal impedance of normalized voltage source = $R\ \Omega$). A similar error model is used for calibration of oneport network analyzer measurements [23].

The *directivity factor* E_D represents systematic errors such as the crosstalk between different channels, the trigger coupling, the reflections of cables and connectors, and so on. There should be no reflections if we measure an ideal 50 Ω load ($S_{\rm dut}^{\rm nor} = 0$). In reality, we measure a certain signal $V_{\rm dut}^{m} = [1 + E_D]U^{\rm nor}$ due to the directivity error factor E_D. The *reflection frequency response factor* E_R (reflection tracking) represents the unwanted filter characteristics of the measurement system (losses in cables, connectors, ...). The measured frequency domain response of an ideal short circuit ($S_{\rm dut}^{\rm nor}) = -1$) will be frequency dependent mainly due to the reflection frequency response factor E_R. The *source impedance match factor* E_S represents the impedance mismatch of the test set-up reflection return port. This error factor causes secondary reflections and disturbs the TDR-pictures. In the literature, long airlines and time domain windowing are quite often used to remove the secondary reflections caused by E_S [13]–[16], [21].

The relation between the measured (superscript"m") frequency domain TDR-picture $V_{\rm dut}^{m} (= [1 + S_{\rm dut}^{m}]U^{\rm nor})$ and the real (superscript"nor") scattering parameter of the DUT $S_{\rm dut}^{\rm nor}$ is given by

$$V_{\rm dut}^{m} = (1 + E_D)U^{\rm nor} + \frac{S_{\rm dut}^{\rm nor} E_R U^{\rm nor}}{1 - E_S S_{\rm dut}^{\rm nor}} = E_D' + \frac{S_{\rm dut}^{\rm nor} E_R'}{1 - E_S S_{\rm dut}^{\rm nor}} \quad (1)$$

where

$$E_D' = (1 + E_D)U^{\rm nor} \quad (2)$$

and

$$E_R' = E_R U^{\rm nor}. \quad (3)$$

As stated before, the secondary reflections caused by the source impedance match error E_S can be neglected by choosing a well-suited (time domain) observation window and by using high-quality delay lines between the DUT and the reflectometer. This simplifies (1) considerably. Quite often however, it is impossible or it is not easy to place airlines between the reflectometer and the DUT. Furthermore, ideal airlines do not exist, and the connectors and/or probes used to connect the airlines may disturb the reflectograms.

Any set of three well-defined broadband calibration standards can be used to characterize the error factors E_D', E_R' and E_S of the frequency domain error model. We can use for example a short circuit ($V_{\rm short}^{m}$), an open circuit ($V_{\rm open}^{m}$) and a 50 Ω load ($V_{\rm load}^{m}$). The better these reference standards are known, the better the systematic errors are compensated. (1) can be rewritten as

$$V_{\rm dut}^{m} = E_D' + (E_R' - E_D' E_S) S_{\rm dut}^{\rm nor} + E_S S_{\rm dut}^{\rm nor} V_{\rm dut}^{m}. \quad (4)$$

This bilinear transformation gives to the following set of equations for SOL- (short, open, load) calibration standards:

$$\begin{pmatrix} V_{\rm short}^{m} \\ V_{\rm load}^{m} \\ V_{\rm open}^{m} \end{pmatrix} = \begin{pmatrix} 1 & S_{\rm short}^{\rm nor} & (V_{\rm short}^{m} S_{\rm short}^{\rm nor}) \\ 1 & S_{\rm load}^{\rm nor} & (V_{\rm load}^{m} S_{\rm load}^{\rm nor}) \\ 1 & S_{\rm open}^{\rm nor} & (V_{\rm open}^{m} S_{\rm open}^{\rm nor}) \end{pmatrix} \begin{pmatrix} E_D' \\ E_R' - E_D' E_S \\ E_S \end{pmatrix} \quad (5)$$

(5) defines the generalised error factors E_D', E_R', and E_S. The reflection coefficients $S^{\rm nor}$ of the reference standards are normaly specified by the manufacturer of the calibration kit. If we use ideal calibration standards we would have $S_{\rm short}^{\rm nor} = -1$, $S_{\rm load}^{\rm nor} = 0$, and $S_{\rm open}^{\rm nor} = 1$.

Once the error network is fully characterized, the normalized TDR-picture $V_{\rm dut}^{\rm nor}$ $(= [1 + S_{\rm dut}^{\rm nor}]U^{\rm nor})$ can be calculated

$$V_{\rm dut}^{\rm nor} = \frac{(V_{\rm dut}^{m} - E_D')U^{\rm nor}}{E_S(V_{\rm dut}^{m} - E_D') + E_R'} + U^{\rm nor}. \quad (6)$$

The corrected reflection coefficient $S_{\rm dut}^{\rm nor}$ of the DUT (reference impedance = $R\ \Omega$) is defined by

$$S_{\rm dut}^{\rm nor} = \frac{(V_{\rm dut}^{m} - E_D')}{E_S(V_{\rm dut}^{m} - E_D') + E_R'}. \quad (7)$$

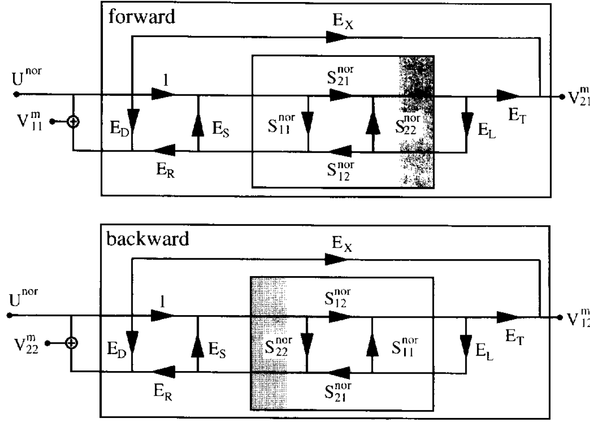

Fig. 4. Flow graph of (a) forward and (b) backward two-port error model.

Note, that the calibration algorithm places the reference plane just in front of the DUT.

C. Twoport Error Model for TDR/T-Measurements

The error model used for twoport measurements is somewhat more complex as the one used for oneport measurements. This extended error model also compensates the unwanted transmission frequency response, the source impedance mismatch, and the crosstalk. It is depicted in Fig. 4. A similar error model is quite often used for the calibration of network analyzer measurements [23]. The twoport frequency domain error model consists of six error terms:

1) E_D the directivity,
2) E_R the reflection frequency response,
3) E_T the transmission frequency response,
4) E_S the source impedance match,
5) E_L the load impedance match,
6) E_X the isolation (leakage).

These parameters can be seen as the S-parameters of the error network (reference impedance = internal impedance of normalized step or pulse generator = R Ω).

The directivity E_D, the reflection frequency response E_R, and the source impedance match E_S error factors were discussed before. The *load impedance match factor E_L* can be compared with the source impedance match factor E_S. E_L describes the impedance mismatch of the transmission return port, while E_S describes the impedance mismatch of the reflection return port of the TDR/T measurement system. These mismatches cause secondary reflections and disturb the TDR/T-pictures. The *transmission frequency response factor* E_T (transmission tracking) can be compared with the reflection frequency response factor E_R. E_T describes the transmission characteristics of the TDR/T-system if $E_D = E_S = E_L = E_X = 0$, while E_R describes the reflection characteristics of such an idealized TDR/T-meter. The *isolation factor E_X* describes the coupling between the source (port 1) and the transmission sampling head (port 2). E_X is also called the crosstalk or the leakage factor.

Four time domain measurements are necessary to fully characterize an unknown twoport DUT, i.e., two reflection measurements and two transmission measurements. First, we perform the forward reflection and transmission measurements (Fig. 4(a)), which results in V_{11}^m and V_{21}^m (after transformation from the time domain to the frequency domain). Then, we rotate the physical DUT over 180°, and we perform the backward measurements (Fig. 4(b)), resulting in V_{22}^m and V_{12}^m. Note that we use a simple measurement set-up which consists of one pulse or step generator and two samplers. The calibration of the (relatively inexpensive) single source TDNA is quite simple, but the measurement of a twoport DUT takes some time. The voltage flow graphs of Fig. 4 show that the relations between the measured voltages V_{ij}^m and the real S-parameters S_{ij}^{nor} $(i, j = 1, 2)$ of the DUT are given by

$$V_{11}^m = E_D' + \frac{E_R'(S_{11}^{\text{nor}} - E_L(S_{11}^{\text{nor}}S_{22}^{\text{nor}} - S_{12}^{\text{nor}}S_{21}^{\text{nor}}))}{1 - E_S S_{11}^{\text{nor}} - E_L S_{22}^{\text{nor}} + E_S E_L(S_{11}^{\text{nor}}S_{22}^{\text{nor}} - S_{12}^{\text{nor}}S_{21}^{\text{nor}})} \tag{8}$$

$$V_{12}^m = E_X' + \frac{E_T' S_{12}^{\text{nor}}}{1 - E_S S_{22}^{\text{nor}} - E_L S_{11}^{\text{nor}} + E_S E_L(S_{11}^{\text{nor}}S_{22}^{\text{nor}} - S_{12}^{\text{nor}}S_{21}^{\text{nor}})} \tag{9}$$

$$V_{21}^m = E_X' + \frac{E_T' S_{21}^{\text{nor}}}{1 - E_S S_{11}^{\text{nor}} - E_L S_{22}^{\text{nor}} + E_S E_L(S_{11}^{\text{nor}}S_{22}^{\text{nor}} - S_{12}^{\text{nor}}S_{21}^{\text{nor}})} \tag{10}$$

$$V_{22}^m = E_D' + \frac{E_R'(S_{22}^{\text{nor}} - E_L(S_{11}^{\text{nor}}S_{22}^{\text{nor}} - S_{12}^{\text{nor}}S_{21}^{\text{nor}}))}{1 - E_S S_{22}^{\text{nor}} - E_L S_{11}^{\text{nor}} + E_S E_L(S_{11}^{\text{nor}}S_{22}^{\text{nor}} - S_{12}^{\text{nor}}S_{21}^{\text{nor}})} \tag{11}$$

where

$$E_T' = E_T U^{\text{nor}} \tag{12}$$

$$E_X' = E_X U^{\text{nor}}. \tag{13}$$

The six generalized error factors $E_D', E_R', E_T', E_S, E_L$ and E_X' are completely defined in an unambiguous way by measuring a set of well-defined broadband SOLT-(Short-Open-Load-Thru) calibration standards, i.e. by four reflection measurements (SOLT) and two transmission measurements (LT). The quality of the definition of the reference standards determines the quality of the calibration. Remark that this calibration method is not restricted to SOLT-standards. We can also use other high-quality broadband reference structures. The calibration procedure proceeds in three steps. *First,* we calibrate the reflection port (port 1) in the same way as we did earlier for reflection measurements. We use a broadband short circuit (0 Ω), a 50 Ω load (match) and an open circuit (∞Ω) as calibration references. The S_{11}^{nor}-parameter of these SOL-standards are specified by the manufacturer of the calibration kit. The relations between the measured voltages V_{11}^m at port 1, and the well-defined reflection coefficients S_{11}^{nor} of the SOL-calibration standards are given by

$$V_{11}^m = E_D' + (E_R' - E_D' E_S) S_{\text{dut}}^{\text{nor}} + E_S S_{\text{dut}}^{\text{nor}} V_{11}^m \tag{14}$$

(14) defines the three generalized error factors E'_D, E'_R, and E_S. In the *second* step, we characterize the generalized isolation factor E'_X. We connect a reference 50 Ω load (match) at both ports of the TDR/T-meter. The small voltage V_{21}^m measured at the second port in transmission is equal to the generalized isolation factor E'_X:

$$V_{21}^m = E'_X. \tag{15}$$

The isolation factor is quite often omitted in literature [24], [25]. In the *third* and last step, we connect both ports of the TDR/T-meter with a reference thru path. The thru path connection is characterized by $S_{11}^{\text{nor}} = S_{22}^{\text{nor}} = 0$ and $S_{12}^{\text{nor}} = S_{21}^{\text{nor}} = e^{-j\omega\tau_D} \approx 1$ (τ_D = time delay). By measuring the reflected voltage V_{11}^m of the thru at port 1 we determine the load impedance match factor E_L from

$$V_{11}^m = E'_D + \frac{E_L E'_R S_{12}^{\text{nor}} S_{21}^{\text{nor}}}{1 - E_S E_L S_{12}^{\text{nor}} S_{21}^{\text{nor}}}. \tag{16}$$

By measuring the transmitted voltage V_{21}^m of the thru at port 2 we determine the transmission frequency response E'_T from

$$V_{21}^m = E'_X + E'_T \frac{S_{21}^{\text{nor}}}{1 - E_S E_L S_{12}^{\text{nor}} S_{21}^{\text{nor}}}. \tag{17}$$

Once the (forward) twoport error model is fully characterized we can calculate the normalized TDR/T-pictures V_{ij}^{nor} $(i, j = 1, 2)$. The relations between the measured and the normalized voltages are given by

$$V_{11}^{\text{nor}} = \left[\left[1 + \left(\frac{V_{22}^m - E'_D}{E'_R}\right) E_S\right]\left(\frac{V_{11}^m - E'_D}{E'_R}\right)\right]\frac{U^{\text{nor}}}{\Delta'} - \left[\left(\frac{V_{21}^m - E'_X}{E'_T}\right)\left(\frac{V_{12}^m - E'_X}{E'_T}\right) E_L\right]\frac{U^{\text{nor}}}{\Delta'} + U^{\text{nor}} \tag{18}$$

$$V_{12}^{\text{nor}} = \left[1 + \left(\frac{V_{11}^m - E'_D}{E'_R}\right)(E_S - E_L)\right]\left(\frac{V_{12}^m - E'_X}{E'_T}\right)\frac{U^{\text{nor}}}{\Delta'} \tag{19}$$

where

$$\Delta' = \left[1 + \left(\frac{V_{11}^m - E'_D}{E'_R}\right) E_S\right]\left[1 + \left(\frac{V_{22}^m - E'_D}{E'_R}\right) E_S\right] - \left[\left(\frac{V_{21}^m - E'_X}{E'_T}\right)\left(\frac{V_{12}^m - E'_X}{E'_T}\right) E_L^2\right]. \tag{20}$$

These equations show that all four voltages V_{ij}^m must be measured to calculate the normalized voltages V_{ij}^{nor} $(i, j = 1, 2)$.

The corrected S-parameters S_{ij}^{nor} (reference impedance = internal impedance of normalized voltage source) can also be written as a function of the generalized error factors $E'_D, E'_R, E'_T, E_S, E_L$ and E'_X, and measured TDR/T-pictures V_{ij}^m $(i, j = 1, 2)$:

$$S_{11}^{\text{nor}} = \left[\left[1 + \left(\frac{V_{22}^m - E'_D}{E'_R}\right) E_S\right]\left(\frac{V_{11}^m - E'_D}{E'_R \Delta'}\right)\right] - \left[\left(\frac{V_{21}^m - E'_X}{E'_T}\right)\left(\frac{V_{12}^m - E'_X}{E'_T}\right)\frac{E_L}{\Delta'}\right] \tag{21}$$

$$S_{12}^{\text{nor}} = \left[1 + \left(\frac{V_{11}^m - E'_D}{E'_R}\right)(E_S - E_L)\right]\left(\frac{V_{12}^m - E'_X}{E'_T \Delta'}\right). \tag{22}$$

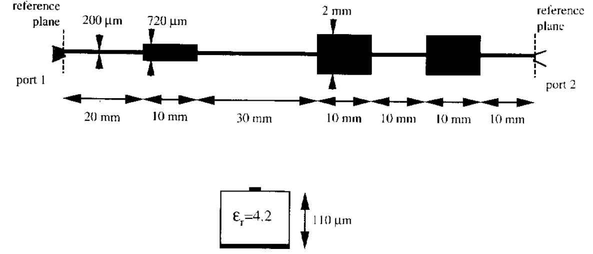

Fig. 5. Top view and cross-section of nonuniform microstrip.

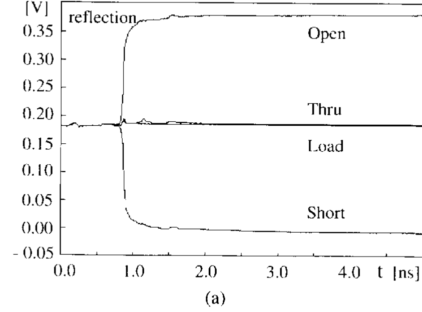

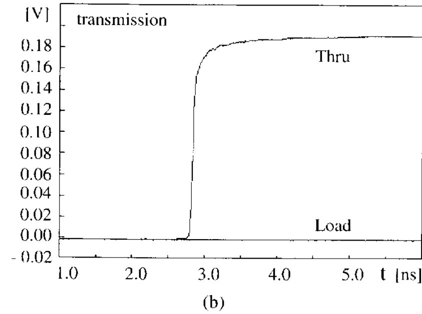

Fig. 6. TDR/T-pictures of reference standards: (a) reflection, (b) transmission.

In the Appendix, simplified error models ($E_S = E_L = 0$) for reflection and transmission measurements are proposed. These models are used in the HP54121T equipment [22].

III. Examples

A. TDR/T-Measurement

As a first example, we examine the time domain reflection and transmission behavior of a multiple step-in-width microstrip structure (two-port measurement). The cross section and the top view of this nonuniform microstrip are depicted in Fig. 5. Both sides of the DUT are connected with the time domain network analyzer via a PCB probing system with coplanar high-frequency probes (Cascade Microtech PPH-100-150 package probe) [30]. These probes ensure a good broadband transition from the coaxial cable to the planar structure up to 12 GHz. Furthermore, we use a HP54121T

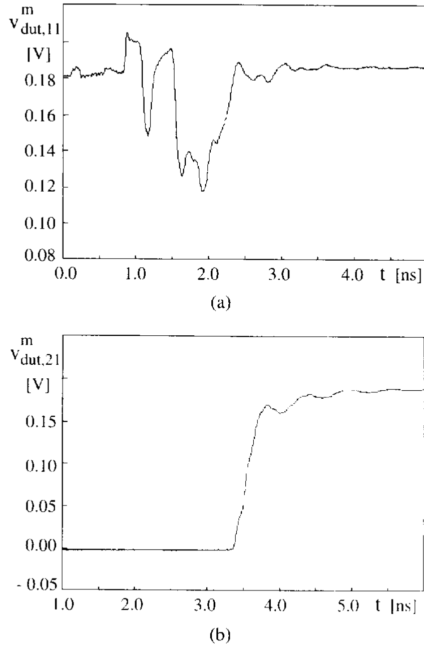

Fig. 7. Measured TDR/T-pictures of the DUT (t_r 38 ps): (a) $v_{11}^m(t)$, (b) $v_{21}^m(t)$.

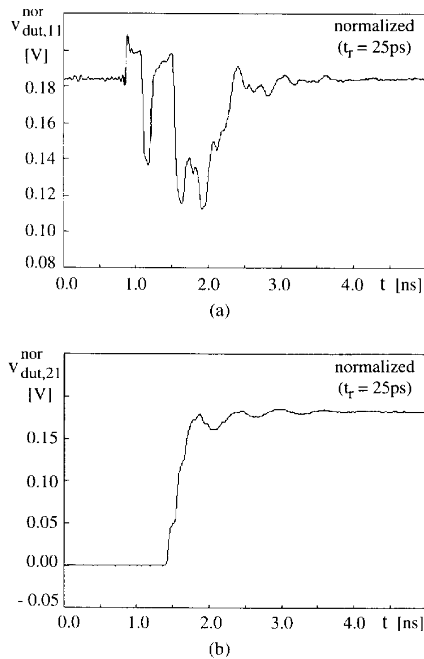

Fig. 8. Normalized TDR/T-pictures of the DUT (t_r = 25 ps): (a) $v_{11}^{nor}(t)$, (b) $v_{21}^{nor}(t)$.

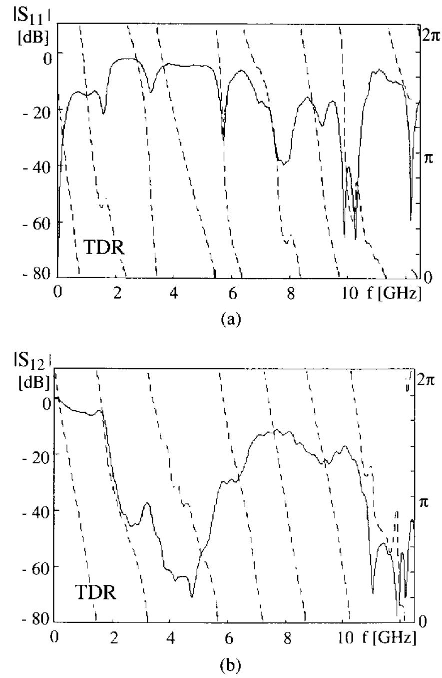

Fig. 9. Amplitude (—) and phase (- - -) of (a)$S_{11}(f)$ and (b) $S_{21}(f)$ measured with a TDR/T-meter (HP54121T) and calculated by TTRECS.

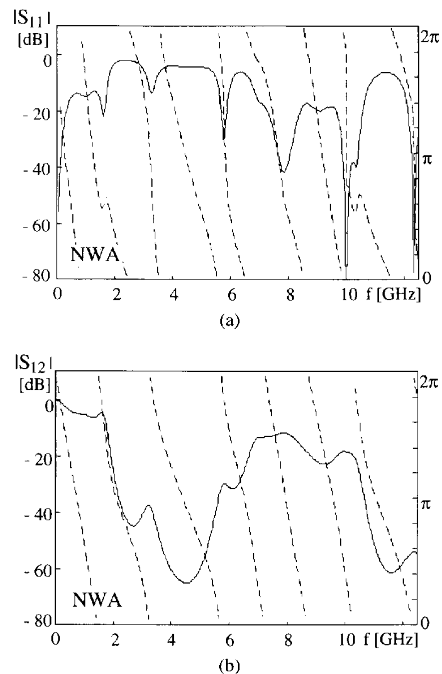

Fig. 10. Amplitude (—) and phase (- - -) of (a)$S_{11}(f)$ and (b) $S_{21}(f)$ measured with a frequency domain network analyzer (HP8510B).

time-domain reflectometer (bandwidth = 18.5 GHz, rise time ≈38 ps), and high-quality 50 Ω coaxial cables.

The 50 Ω impedance, the short circuit, the open circuit and the thru on the Cascade Microtech "Impedance Standard Substrate" (ISS) are used to calibrate the TDNA. The calibration standards on this alumina substrate are well known and clearly described [22]. In Fig. 6(a) and (b), the TDR-pictures

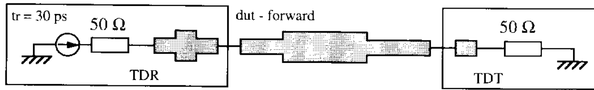

Fig. 11. TDR/T set-up for two-port measurements.

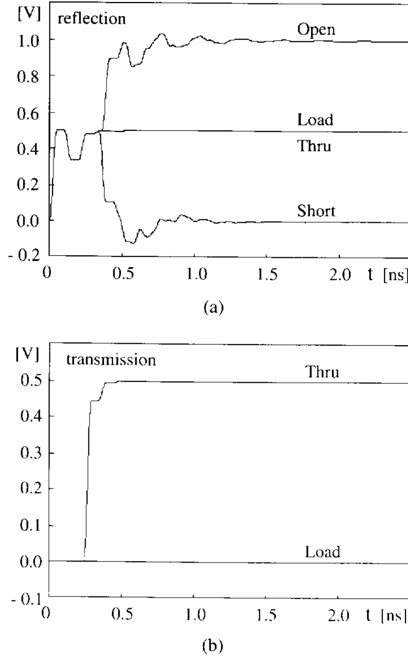

Fig. 12. TDR/T-pictures of reference standards (t_r = 30 ps): (a) reflection, (b) transmission.

of the reference standards are shown. Waveform averaging is used (128 times) to improve the signal/noise ratio. The disturbances caused by the probe transition can be seen. Based on the reference standards, a (frequency domain) digital filter is created.

The uncalibrated "raw" time-domain measurement of the DUT is shown in Fig 7. The normalized (rise time of 25 ps) TDR-picture is shown in Fig. 8. We reduced the rise time significantly (38 ps $\rightarrow$ 25 ps). The software package TTRECS also calculates the scattering parameters of the DUT. The amplitude and the phase of the S-parameters $S_{11}(f)$ and $S_{21}(f)$ (reference impedance = 50 Ω) are depicted in Fig. 9. They correspond very well with the network analyzer measurements (HP8510B) which are shown in Fig. 10 (both in amplitude and phase). The dynamic range of the time domain network analyzer is about 40 dB.

B. TDR/T-Simulation

As a second example, we verify the correctness of the twoport calibration and normalization procedure. The TDR/T-pictures are simulated with the transient simulator TMSIM [31]. No noise was added. This approach makes it possible to evaluate the accuracy of the calibrated S-parameters, and the correctness of the normalized reflected and transmitted signals. The bandwidth of the TDR/T-pictures is limited (Nyquist criterion) by the finite time step of the simulation (Δt = 1 ps).

The TDR/T set-up is shown in Fig. 11. The DUT is an asymmetric double step-in-width microstrip line (which consists of three transmission lines with different impedance and with different delay time: 50 Ω /100 ps + 25 Ω/220 ps + 50 Ω/140 ps). The transmission port (port 2) of the time domain network analyzer is perfectly matched (50 Ω/50 ps + 50 Ω). The reflection port (port1) consists of an ideal voltage source (amplitude = 1 V, rise time = 30 ps, internal impedance = 50 Ω) and a double step-in-width transmission line (50 Ω/50 ps + 25 Ω/50 ps + 50 Ω/50 ps). This nonuniform transmission line of the first port causes secondary reflections and disturbs all TDR/T-pictures. The software package TTRECS is used to remove the unwanted effects caused by the non-ideal ports.

First, we characterize the twoport error model associated with this TDR/T measurement set-up. The TDR/T-pictures of the four SOLT reference standards, i.e. a short circuit (50 Ω/20 ps + 0 Ω), an open circuit (50 Ω/30 ps + ∞Ω) a load (50 Ω), and a thru (50 Ω/40 ps) are shown in Fig. 12 (rise time = 30 ps). The frequency dependent factors of the twoport error model are calculated with the new software package TTRECS. As expected, E_X and E_L are equal to zero. The other error factors are shown in Fig. 13 as a function of frequency.

Once the error model is fully characterized, we normalize the TDR/T pictures and calculate the calibrated scattering parameters. The "raw" TDR/T-pictures of the DUT are depicted in Fig. 14 (rise time = 30 ps). The software package TTRECS is used to normalize these time domain signals to different rise times. The (shifted) results are depicted in Fig. 15 (rise time = 5 ps, 30 ps, 100 ps and 300 ps). The secondary reflections caused by the imperfect TDR/T-system are mathematically removed! The corrected and normalized voltage waves (calculated with TTRECS) correspond very well with the simulated results (calculated with the transient simulator TMSIM) of the idealized TDR/T-system (with ideal ports). Note that the noise content of the time domain signals increases if the rise time decreases or if the bandwidth increases ("pumped up"). In Fig 16, the amplitude and the phase of the scattering parameters $S_{11}(f)$ and $S_{21}(f)$ (calculated with TTRECS) are shown. They correspond very well with the S-parameters of the DUT calculated with the Microwave Design System (MDS) of Hewlett Packard (HP54150). In Fig. 17, we compare the normalized TDR/T-pictures (t_r = 30 ps) calculated with TTRECS and with the simplified error models used in [21] (no airlines).

IV. Conclusion

In this paper we presented a new software package TTRECS for the calibration and normalization of a time domain network analyzer. We use a simple measurement set-up which consists of one source and two samplers. Frequency domain error models are used to correct the TDR/T-measurements. These error models are fully characterized by measuring a set of precisely known (SOLT-) calibration standards. TTRECS calculates normalized TDR/T-pictures as well as calibrated S-parameters. First, the discretized measured time domain

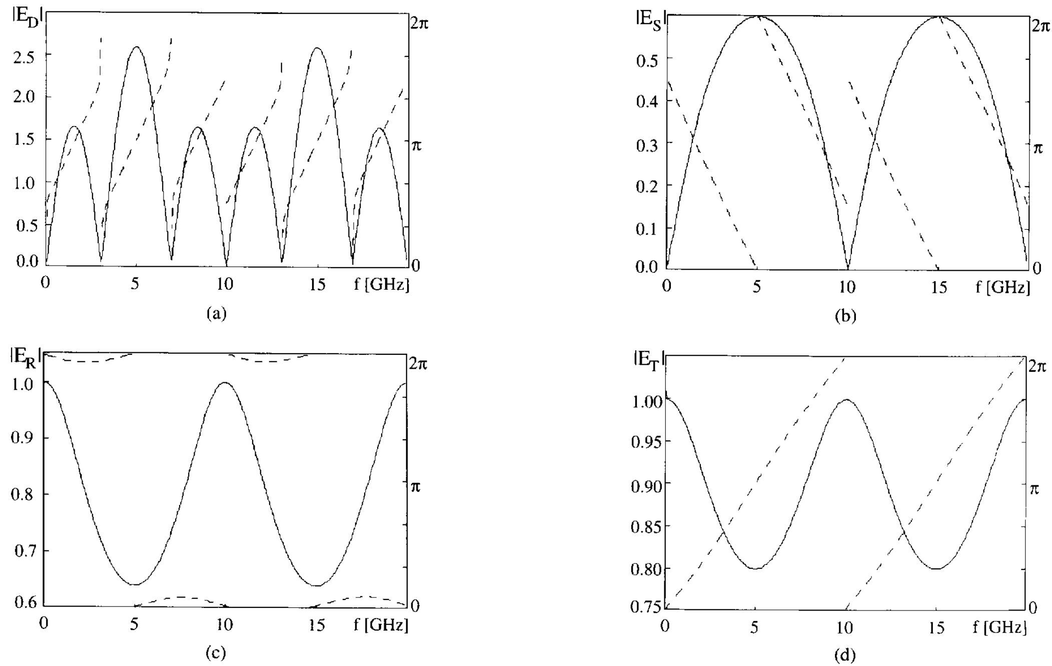

Fig. 13. Error factors as a function of frequency of the twoport error model (a) $E_D(f)$, (b) $E_S(f)$, (c)$E_R(f)$, (d) $E_T(f)$ [amplitude (—) and phase (- - -)].

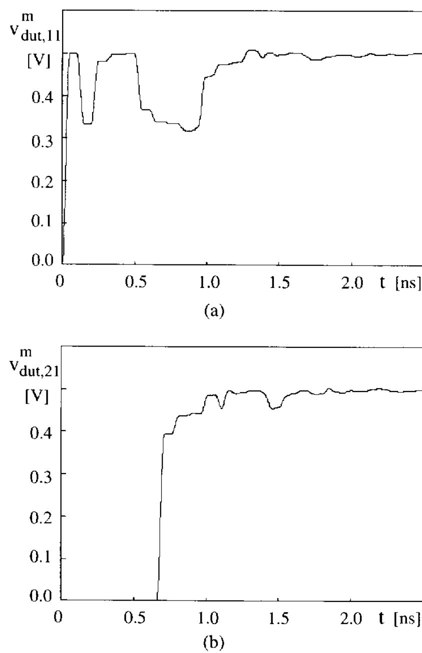

Fig. 14. TDR/T-pictures of DUT (t_r = 30 ps): (a)$v^m_{11}(t)$, (b) $v^m_{21}(t)$

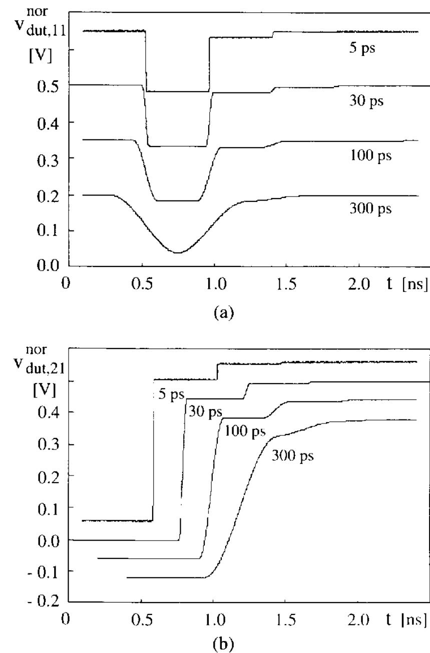

Fig. 15. Normalized TDR/T-pictures (t_r = 5 ps, 30 ps, 100 ps, 300 ps): (a) $v^{nor}_{11}(t)$, (b) $v^{nor}_{21}(t)$.

signals are transformed to the frequency domain. Then, the frequency domain data are corrected mathematicaly and the S-parameters of the DUT are calculated. Afterwards, the corrected data are transformed back to the time domain, which results in normalized TDR/T-pictures.

Appendix
Simplified Error Models

The calibration and normalization procedure of the HP-54121T TDR/T measurement system [22] is based on simpli-

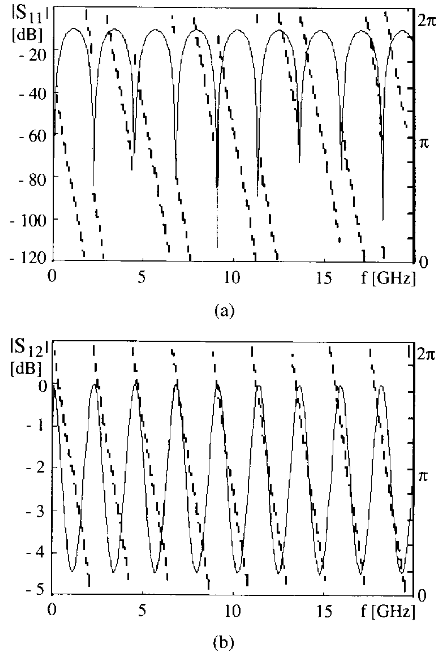

Fig. 16. Amplitude (—) and phase (- - -) of S-parameters (a) S_{11} and (b) S_{21} calculated by TTRECS.

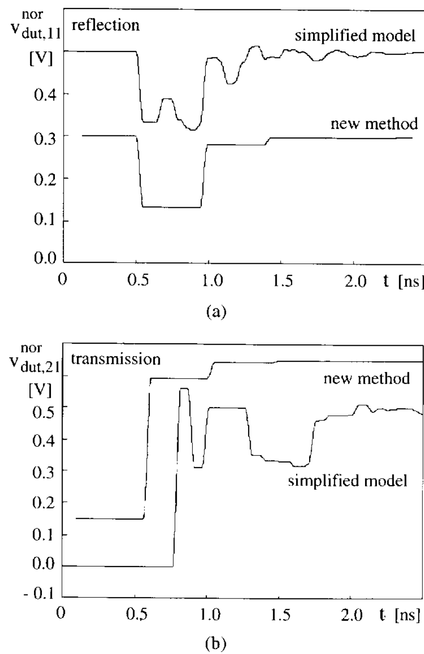

Fig. 17. Comparison between the normalized TDR/T-pictures (t_r = 30 ps) calculated with the new method and a simplified method [21]: (a) $v_{11}^m(t)$, (b) $v_{21}^m(t)$

fied frequency domain error models. All reference calibration standards are idealized. Time domain windows and long ideal airlines are used to avoid secondary reflections. As stated earlier, sometimes it is impossible or very difficult

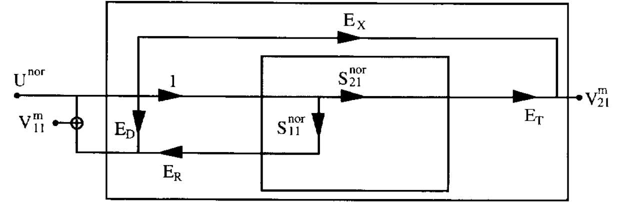

Fig. 18. Flow graph of simplified two-port error model.

to place airlines between the TDR/T-system and the DUT, and the airlines and their connectors will introduce some supplementary unwanted reflections and filtering.

A. Reflection Measurements

The source impedance match factor E_S is neglected in the simplified reflection error model. Only two idealized reference standards are used to characterize this error network (a short and a 50 Ω load). In that case, the normalized TDR-picture is defined as

$$V_{11}^{\mathrm{nor}} = \left[\frac{(V_{\mathrm{short},11}^{\mathrm{nor}} - U^{\mathrm{nor}})}{(V_{\mathrm{short},11}^{m} - V_{\mathrm{load},11}^{m})} (V_{11}^{m} - V_{\mathrm{load},11}^{m}) \right] + U^{\mathrm{nor}} \tag{A.1}$$

The corrected reflection coefficient S_{11}^{nor} (reference impedance = internal impedance of idealized source) is

$$S_{11}^{\mathrm{nor}} = \frac{(S_{11}^m - E_D)}{E_R} = -\frac{(V_{11}^m - V_{\mathrm{load},11}^m)}{(V_{\mathrm{short},11}^m - V_{\mathrm{load},11}^m)} \tag{A.2}$$

B. Transmission Measurements

The simplified transmission error model is depicted in Fig. 18. The source impedance match factor E_S and the load impedance match factor E_L are neglected. Note that the reflection and the transmission measurement are now completely uncoupled. Two idealized reference standards are used to characterize the "transmission"-part of the error network (a thru and a load). In that case, the normalized TDT-picture is defined as

$$V_{21}^{\mathrm{nor}} = \frac{(V_{21}^m - V_{\mathrm{load},21}^m)}{(V_{\mathrm{thru},21}^m - V_{\mathrm{load},21}^m)} V_{\mathrm{thru},21}^{\mathrm{nor}} \tag{A.3}$$

The corrected transmission coefficient S_{21}^{nor} (reference impedance = internal impedance of idealized source and sampler) is

$$S_{21}^{\mathrm{nor}} = \frac{(S_{21}^m - E_X)}{E_T} = -\frac{(V_{21}^m - V_{\mathrm{load},21})}{(V_{\mathrm{thru},21}^m - V_{\mathrm{load},21}^m)} \tag{A.4}$$

Acknowledgment

The authors gratefully acknowledge the contribution of Kurt De Kesel, Mieke Herreman and Peter Degraeuwe in the preparation of the measured data.

References

[1] R. Y. Yu, M. Kamegawa, M. Case, M. J. W. Rodwell, and J. Franklin, "A 2.3 ps time-domain reflectometer for millimeter-wave network analysis," *IEEE Microwave Guided Wave Lett.*, vol. 1, pp. 334–336, Nov. 1991.

[2] J. Rohrig, "Location of faulty places by measuring with cathode ray oscillographs," *Elektrotech. Z.,* vol. 8, pp. 241–242, Feb. 1931.

[3] U. Piller, "Time domain immittance measurements," *4th European Microwave Conference,* Montreux, Switzerland, September 1974, pp. 61–65.

[4] S. M. Riad, "Modeling of the HP-1430A feedthrough wide-band (28-ps) sampling head," *IEEE Trans. Instrument. Measurement,* vol. IM-31, no. 2, pp. 110–115, June 1982.

[5] S. T. Salvage, B. Parruck, and S. M. Riad, "Wide-band device modeling using time-domain reflectometry," *IEEE Trans. Instrument. Measurement,* vol. IM-32, no. 1, pp. 134–136, Mar. 1983.

[6] J. Chilo and G. Angenieux, "Effects of interconnection lines in very high speed packaging for digital applications," *The Int. J. Hybrid Microelectron.,* vol. 12, no. 3, pp. 134–136, Sept. 1989.

[7] M. S. Lin, A. H. Engvik, and J. S. Loos, "Measurements of transient response on lossy microstrips with small dimensions," *IEEE Trans. Circuits Syst.,* vol. 37, pp. 1383–1393, Nov. 1990.

[8] W. Su, S. M. Riad, T. Poulin, D. Fett, and Z.-Y. Shen, "Wideband characterization and modeling of TAB packages using time-domain methods," *Int. J. Hybrid Microelectron.,* vol. 14, no. 2, pp. 55–61, June 1991.

[9] A. Deutsch, G. Arjavalingam, and G. V. Kopcsay, "Characterization of resistive transmission lines by short-pulse propagation," *IEEE Microwave Guided Wave Lett.,* vol. 2, pp. 25–27, January 1992.

[10] K. M. Fidanboylu, S. M. Riad, and A. Elshabini-Riad, "An enhanced time-domain approach for dielectric characterization using stripline geometry," *IEEE Trans. Instrument. Measurement,* vol. 41, pp. 132–136, Feb. 1992.

[11] J. M. Jong, V. K. Tripathi, and B. Janko, "Circuit modeling of high speed packages from TDR/T measurements," *Topical Meeting on Electrical Performance of Electronic Packaging,* Tucson, Arizona, April 1992, pp. 150–153.

[12] M. Sipilä, K. Lehtinen, and V. Porra, "High-frequency periodic time-domain waveform measurement system," *IEEE Trans. Microwave Theory Tech.,* vol. MTT-36, pp. 1397–1405, Oct. 1988.

[13] A. M. Nicolson, C. L. Bennett, Jr., D. Lamensdorf, and L. Susman, "Applications of time-domain metrology to the automation of broad-band microwave measurements," *IEEE Trans. Microwave Theory Tech.,* vol. MTT-20, pp. 3–9, Jan. 1972.

[14] J. R. Andrews, "Automatic network measurements in the time domain," *Proc. IEEE,* vol. 66, pp. 414–423, Apr. 1978.

[15] N. S. Nahman, J. R. Andrews, W. L. Gans, M. E. Guillaume, R. A. Lawton *et al.*, "Applications of time-domain methods to microwave measurements," *IEE Proc.,* vol. 127, Pt. H, pp. 99–106, Apr. 1980.

[16] P. R. Rigg and J. E. Carroll, "Low-cost computer-based time-domain microwave network analyzer," *IEE Proc.,* vol. 127, Pt. H, pp. 107–111, Apr. 1980.

[17] W. R. Scott, Jr. and G. S. Smith, "Error corrections for an automated time-domain network analyzer," *IEEE Trans. Instrument. Measurement,* vol. IM-35, pp. 300–303, Sept. 1986.

[18] ——, "Corrections to "Error corrections for an automated time-domain network analyzer," *IEEE Trans. Instrument Measurement,* vol. IM-37, pp. 163, Mar. 1988.

[19] W. Su and S. M. Riad, "Time domain calibration of TDR measurement system," *Conf. Precision Electromag. Measurements,* pp. 1451–1454, July 1992.

[20] Hewlett Packard, "TDR fundamentals for use with HP 54121T digitizing oscilloscope and TDR," HP-Appl. Note 62.

[21] ——, "Improving the time domain network analysis measurements for use with HP 54121T digitizing oscilloscope and TDR," HP-Appl. Note 62-1.

[22] ——, "Advanced TDR techniques," HP-Appl. Note 62-3, May 1990.

[23] J. Williams, "Accuracy enhancement fundamentals for vector network analyzers," *Microwave J.,* pp. 99–114, Mar. 1989.

[24] L. A. Hayden and V. K. Tripathi, "Thru-match-short calibration for time domain network analyzers," *IEEE Microwave Theory Tech. Symp.,* Albuquerque, NM, June 1992, pp. 1447–1450.

[25] P. Ferrari, G. Angénieux, and B. Fléchet, "A complete calibration procedure for time domain network analyzers," *IEEE Microwave Theory Tech. Symp.* Albuquerque, NM, July 1992, pp. 1451–1454, .

[26] T. Dhaene, L. Martens, P. Degraeuwe, and D. De Zutter, "Improved time-domain characterization of high-speed interconnection structures," *Topical Meeting on Electrical Performance of Electronic Packaging,* Tucson, Arizona, April 1992, pp. 142–144.

[27] G. D. Cormack, D. A. Blair, and J. N. McMullin, "Enhanced spectral resolution FFT for step-like signals," *IEEE Trans. Instrument. Measurement,* vol. 40, pp. 34–36, Feb. 1991.

[28] F. J. Harris, "On the use of windows for harmonic analysis with the discrete fourier transform," *Proc. IEEE,* vol. 66, pp. 51–83, Jan. 1978.

[29] T. Dhaene, L. Martens, and D. De Zutter, "Generalized iterative frequency domain deconvolution technique," *IMTC/93,* Irvine, CA, pp. 85–87, May 1993.

[30] P. Degraeuwe, L. Martens, and D. De Zutter, "Measurement Set-up for high-frequency characterization of planar contact devices," *39th ARFTG Conf. Dig.*, Albuquerque, NM, July 1992, pp. 19–25.

[31] T. Dhaene, L. Martens, and D. De Zutter, "Transient simulation of arbitrary nonuniform interconnection structures characterised by scattering parameters," *IEEE Trans. Circuits Syst.,* vol. 39, pp. 928–937, Nov. 1992.

Tom Dhaene was born in Deinze, Belgium, on June 25, 1966. He received the degree in electrical engineering from the University of Ghent, Belgium, in 1989. He is currently working towards the Ph. D. degree in electrical engineering at the Laboratory of Electromagnetism and Acoustics (LEA) of the same university.

His research focuses on all aspects of circuit modeling, transient simulation and time domain charcterization of high-frequency and high-speed interconnections.

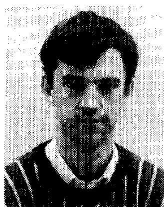

Luc Martens was born in Ghent, Belgium on May 14, 1963. He received the degree and the Ph.D. degree in electrical engineering from the University of Ghent in 1986and 1990, respectively.

From September 1986 to December 1990, he was a Research Assistant in the Laboratory of Electromagnetism and Acoustics at the University of Ghent.. During this period, his scientific work was focussed on the physical aspects of hyperthermic cancer therapy. His research work dealt with electromagnetic and thermal modeling and with the development of measurement systems for that application. Since April 1993, he has been a Professor at Ghent University.

Daniël De Zutter, for a photograph and biography see page 513 of the March issue of this TRANSACTIONS